A major purpose of the Technical Information Center is to provide the broadest dissemination possible of information contained in DOE's Research and Development Reports to business, industry, the academic community, and federal, state and local governments.

Although a small portion of this report is not reproducible, it is being made available to expedite the availability of information on the research discussed herein.

1

LA-UR -83-2949

CONF-831043--9

Los Alamos National Laboratory is operated by the University of California for the United States Department of Energy under contract W-7405-ENG-36.

LA-UR--83-2949

DE84 001718

TITLE: TRAC ANALYSES FOR CCTF AND SCTF TLSTS AND UPTF DESIGN/OPERATION

AUTHOR(S): K. A. Williams

NOTICE

PORTIONS OF THIS REPORT ARE ILLEGIBLE.

It has been reproduced from the best available copy to permit the broadest possible availability.

SUBMITTED TO: 11th Water Reactor Safety Research Information Meeting, October 25 - 27, 1983, Gaithersburg, MD.

Los Alamos

Los Alamos National Laboratory
Los Alamos, New Mexico 87545

FORM NO 836 R4
ST NO 2629 5/81

TRAC ANALYSES FOR CCTF AND SCTF TESTS AND UPTF DESIGN/OPERATION*

by

K. A. Williams
Principal Investigator
Energy Division
Los Alamos National Laboratory
Los Alamos, New Mexico 87545

The 2D/3D Program is a multinational (Germany, Japan, and the United States) experimental and analytical nuclear reactor safety research program. Its main objective is investigation of multidimensional, nonequilibrium thermal-hydraulic behavior in large-scale experimental test facilities having hardware prototypical of pressurized water reactors (PWRs). The Japanese are presently operating two large-scale test facilities as part of this program: the Cylindrical Core Test Facility (CCTF) and the Slab Core Test Facility (SCTF). The CCTF is a 2000-electrically-heated-rod, cylindrical-core, four-loop facility with active steam generators primarily used for investigating integral system reflood behavior. The SCTF is a 2000-electrically-heated-rod, slab-core (one fuel assembly wide, eight across, and full height), separate-effects reflood facility. Both facilities have prototypic power-to-volume ratios, preserving full-scale elevations, and are much larger than any existing facilities in the United States (including LOFT). The German contribution to the program is the planned Upper Plenum Test Facility (UPTF), a full-scale facility with vessel, four loops, and a steam-water core simulator. All of these facilities have more instruments than any existing facilities: conventional instrumentation data channels alone are in excess of one thousand in each facility. The United States contributions to the program are the provision of advanced two-phase flow instrumentation and analytical support.

The Los Alamos National Laboratory is the prime contractor to the NRC in the latter activity. The main analytical tool in this program is the Transient Reactor Analysis Code (TRAC), a best-estimate, multidimensional,

*Work performed under the auspices of the US Nuclear Regulatory Commission.

nonequilibrium, thermal-hydraulics computer code developed for the NRC at Los Alamos. Through code predictions of experimental results and calculations of PWR transients, TRAC provides the analytic coupling between the facilities and extends the results to predicting actual PWR behavior.

Results from this program already have addressed, and will continue to address, key licensing issues including: scaling, multidimensional effects, downcomer bypass and refill, reflood, steam binding, core blockages, alternate emergency core cooling systems (ECCS), and code assessment.

During the previous year, the application of TRAC-PF1 to the 2D/3D program was highlighted by fine-node, large-break loss-of-coolant-accident (LOCA) calculations of both the US/Japanese and German PWR reference reactors. The calculations utilized new input models that more correctly represent plant geometry and operating conditions; for the US/Japanese PWR the input model was based upon the newer Westinghouse 17x17 type plants. These LOCA analyses included a double-ended (200%) cold-leg break for both the Westinghouse plant and the German Kraftwerk Union (KWU) combined ECC injection plant. A (200%) hot-leg break LOCA calculation was also completed for the KWU plant.

A Westinghouse 3411 MWt PWR with 17x17 fuel assemblies twelve feet in length was selected as the reference US PWR for this best-estimate LOCA calculation. The TRAC input model was derived from actual plant data provided by Westinghouse Electric Corporation. A schematic of the complete system model used for the transient calculation is shown in Fig. 1. All the loop components such as the hot leg, steam generator, loop seal, circulating pump, cold leg and emergency core cooling system (ECCS) were modeled as physically complete as possible. A schematic of the vessel component is shown in Fig. 2. The vessel has been subdivided into 17 axial levels, 4 radial rings and 8 azimuthal sectors for a total of 544 hydrodynamic cells. The core region consists of the 2 inner radial rings and the 5 axial levels extending between levels 4 to 9. The barrel baffle region extends from level 4 to 10 and occupies the 3rd radial ring within these levels. The fourth radial ring represents the downcomer region from level 3 to 15. At the top of level 15 in each azimuthal sector open flow area passages are located to model the upper head spray nozzles. Flow paths between the upper head and upper plenum were represented by the modeling of the control rod guide tubes that traversed these two regions. These guide tubes were modeled with pipe components within the vessel. Three guide tubes were combined for each sector of the inner ring and 4.5 guide tubes for each sector of the outer ring.

This PWR analysis simulates a 200% guillotine break of a cold leg. The break is located between the cold leg nozzle and the ECC injection port immediately outside of the biological shield. The system model consists of 953 hydrodynamic fluid cells and is considered to be a very finely noded model. This "best-estimate" calculation based on most-probable plant conditions provides insight into the thermal-hydraulic response of the PWR system during a transient, particularly during the vessel refill and reflood phases of the transient. The sequence of events is given in Table I.

The important conclusions of this analysis are:

1. Peak clad temperature of 810 K (999^{O}F) for the highest powered rod occurred during blowdown at 2.5 s [775 K (935^{O}F) for an average powered rod].
2. Blowdown ended at 26 s.
3. Lower plenum refilled at 37 s (reflood initiated).
4. Accumulator nitrogen entering the vessel at 57 s caused a more rapid reflood of the core.
5. Significant multidimensional effects were calculated to occur in the vessel.
6. Core region completely quenched by 89 s.

The predicted cladding temperature response of a high powered rod (8.63 kw/ft local peak) is shown in Fig. 3. This figure shows the temperature transient at six axial elevations measured from the bottom of the heated core. The rapid cooldown of the entire rod during the first few seconds of the transient is due to a rapid refilling of the core, shown in Fig. 4. The core flow returned to positive because the mass flow from the three intact loops (with pumps spinning) exceed the choked flow out the single broken loop. The fuel rods continued to cool until 20 to 25 s into the transient. This longer term cooling resulted partially from the blowdown of the upper head water through the control rod guide tubes. Although a reheat of the core occurred during the refill/reflood phase, the maximum temperature never exceed the earlier blowdown peak of 810 K (999°F). During the core reflood phase there were significant manometer-type oscillations between the core and downcomer. The core inlet mass flow is shown in Fig. 5. These oscillations were predicted, primarily because of the very short time (60 s) required to reflood and quench the entire core. This calculation also modeled the noncondensible gas (nitrogen) field that entered the system after all accumulator water was discharged. When nitrogen entered the system at 56 s it pressurized the upper downcomer region and locally lowered the condensation rates. This increased the core reflooding rate and damped the manometer oscillations after nitrogen was in the primary system.

The calculation of a 200% cold-leg break in the GPWR also showed that the peak clad temperature occurred early in the blowdown phase and that the entire core was quenched within 80 s. These results were presented at last years meeting.

The calculation of a 200% hot-leg break in the GPWR was uneventful. That is, the fuel rods immediately cooled down from the beginning of the transient due to a large positive core flow. Although there was a dryout reheat during refill, the peak clad temperature never exceeded the initial steady state value.

For the CCTF Core-II, analyses were provided for the base case test (Run 53) as well as for some of the parametric effects tests. These included the low core stored energy test (Run 51) and the flat radial power test with lower power (Run 64). The objectives of Run 51 were to check the functions of the modified CCTF Core-II facility, confirm the similarities between the Core-I and Core-II test facilities, and to study the effect of low initial clad temperature (core stored energy). With the exception of the initial clad temperature and radial power profile, the test conditions are identical to those of the base case test of Core-II (C2-SH1, Run 53). The overall schematic of the TRAC CCTF model is shown in Fig. 6. Input modeling changes that were necessitated by differences between Cores I and II in the CCTF facility are included in this calculation. Like previous coarse-node CCTF calculations, the three intact loops are combined into one, and the broken loop is modeled separately.

The overall vessel noding is shown in Fig. 7. This new configuration, called the intermediate-node model, represents a compromise between the coarse and fine-node models previously used in the CCTF calculations. The coarse-node model, which lumps all 900 rods in one half of the core into one average rod, fails to account for the extremely steep radial power profile from the high-to-low power regions of the core for this test (1.51:1.1.14:0.77). The intermediate-node model was created to resolve this problem by dividing the vessel radially into four sections. The outer radial section models the downcomer and the inner three sections represent the three power regions of the CCTF core. The TRAC calculation was performed in manner analogous to the actual test. Starting from the initial conditions there was a constant power heatup for 54 s. Accumulator injection into th lower plenum began at 45 s into the test, and continued until water began to penetrate the core. A power decay was initiated at bottom-of-core-recovery (BOCREC). The ECC injection was switched from the lower plenum to the intact cold leg at 56.5 s, and then switched from the accumulators to the LPCI at 69 s. This LPCI injection flow continued until all rods were quenched.

Accumulator injection into the lower plenum begins at 45 s. The lower plenum fills rapidly and remains full for the remainder of the transient. Unlike previous TRAC-PD2 calculations which predict a rapid increase in the lower plenum liquid temperature to saturation, in the TRAC-PF1 calculation the liquid remains subcooled for most of the transient, eventually reaching the saturation temperature at 580 s.

The core liquid mass (Fig. 8) oscillates $\pm$50 kg shortly after BOCREC, but nonetheless fills rapidly as the downcomer head forces the lower plenum liquid into the core. The liquid mass peaks at 450 kg, and then declines as the downcomer head decreases. It recovers to 400 kg and then declines again as the downcomer head is further reduced by boiling. After 160 s, the core mass gradually increases (with minor oscillatory behavior) to 550 kg at the end of the transient. The CCTF core mass curve shown in Fig. 8 was made using JAERI core differential pressure data and converting it to liquid mass using the relation $m = \Delta PA/g$, where g is the gravitational constant and A the core flow area. This expression assumes that the core pressure drop is due entirely to the core static liquid head. A direct comparison of the TRAC prediction to the CCTF data shows the CCTF core initially filling faster than TRAC predicts, but leveling off at 300 kg. This time difference is due to the oscillatory behavior predicted by TRAC after the core begins to fill. CCTF data indicate fewer initial oscillations and hence faster core filling. The core voiding after the initial peak that was predicted by TRAC is not seen in the CCTF data which gradually increases with time to 375 kg. This causes an average mass difference between the TRAC prediction and CCTF data of approximately 100 kg (corresponding to a 2.4 kPa pressure difference) for the duration of the transient. The downcomer fills rapidly during this period and reaches a peak liquid mass of 1444 kg at 75 s (Fig. 9). This mass immediately decreases to 1100 kg, indicating that the downcomer filled above the nozzle level, and drained the excess 344 kg out through the broken cold leg. The average temperature of the downcomer liquid increases rapidly due to the heat transfer from the downcomer walls. The downcomer liquid begins to boil as the saturation temperature is approached at 110 s, thereby accounting for the sharp decline in liquid to 800 kg. As the stored energy in the downcomer walls dissipates, the downcomer slowly begins to fill again, until a liquid mass of 1150 kg is attained at the end of the transient.

The TRAC-PF1 predicted cladding temperature responses at five axial elevations along a medium powered rod are compared to CCTF data in Fig. 10. The thermocouple elevations are measured from the bottom of the vessel. Since the bottom of the heated length is at 2.1 m the TRAC 2.48 location is 0.38 m into the core. The TRAC values (shown as solid lines) exhibit an early cooldown not seen in the data; this is due to an initial temporary surge of liquid through the core. The peak temperatures are predicted to within 50^{o}C at all elevations and the subsequent cooldown rate is in reasonable agreement with the CCTF data. The progression of the quench front is shown in Fig. 11. to be in very good agreement with the measured quenching behavior.

Although agreement between the TRAC calculation and Run 51 test results were good, TRAC underpredicted the core flooding rate. It was shown that this underprediction was due in part to the low downcomer head due to excess vapor generation from the hot walls. This resulted in a lower core average pressure, a lower core heat transfer rate, lower loop differential pressures and mass flows, and a longer quenching time at the upper rod elevations. Steam binding in both the intact and broken loop steam generators was not calculated to take place as no liquid exited the vessel through the hot legs. This had the effect of further reducing loop mass flows, accounting for the lower differential pressures predicted by TRAC. In addition, the large manometer oscillations damped out quickly and afterwards had no further effect on system behavior. The initial water excursion into the core quenched all rods at the lower elevations quickly and cooled the medium and high powered rods to temperatures below that observed in the CCTF. In general, the rods quenched early in the bottom half of the core, on time at the midplane, and slightly late at the upper core elevations. Both the CCTF data and the TRAC calculation showed that the low stored energy test quenched earlier than did the base case test.

During this year the SCTF test series and analyses covered gravity driven reflood operation for the first time. TRAC aided in the selection of proper boundary/initial conditions for these tests. A TRAC prediction was provided for the base case gravity reflood test having cold-leg ECC injection, Run 537. Since the JAERI magnetic data tape has not yet arrived at Los Alamos, it is not possible to show direct comparisons between experimental and analytical results. However, a qualitative overview of the transient is given in Figs. 12, 13, and 14. The vessel filling hydraulics are shown by the calculated downcomer liquid mass (Fig. 12) and core liquid mass (Fig. 13). It can be concluded from these figures (and JAERI "quick-look" plots) that this SCTF gravity reflood test proceeded in a relatively smooth manner and is qualitatively similar to CCTF tests conducted under similar conditions. The heater rod surface thermal response is shown in Fig. 14 at ten axial elevations (measured in meters above the bottom of the heated length). Again, the SCTF response is typical of results from the integral facility CCTF. This test has demonstrated that the SCTF can be successfully operated in a gravity reflood mode. This analysis has demonstrated that TRAC can help select proper test operating conditions and can correctly predict transient behavior in gravity driven SCTF tests.

Previous SCTF tests in the forced-injection power shape test series had shown experimentally that multidimensional effects were very important in the reflood thermal-hydraulics. Los Alamos 2D/3D staff developed a procedure for evaluating the rod bundle cross-flow resistance to be used in the TRAC input model. This same procedure was used in the PWR plant calculations. To assess the effects of this model, a recalculation was made of SCTF Run 514, the steep radial power shape test. This calculation showed that although the bundle-to-bundle cross-flow had been reduced from the previous TRAC calculation, the transient results were still in good agreement with the experiment due to an increased "chiminey effect" above the quench front in the high power bundles.

A total of six design/operation studies for the UPTF were conducted with TRAC during the previous year. These efforts focused on calculating the overall system behavior of the UPTF. A large effort was needed to develop the UPTF system input model, especially the TRAC modeling of the core simulator and its feedback control system. The first design study checked out this modeling with a simple one-dimensional vessel model. The second study was a complete UPTF system calculation but with preprogrammed core simulator flows. The third design study used base case conditions as originally specified by FRG and with core simulator feedback control. As a result of this calculation it was decided that the lower plenum initial liquid inventory needed to be reduced. The fourth and fifth calculations investigated the sensitivity of this liquid inventory. The sixth calculation simulated 40 s of UPTF transient time and assumed no liquid inventory in the secondary side of the broken loop steam/water separators. The objective of these studies was to determine how to operate UPTF so as to best simulate an actual GPWR LOCA transient. The German KWU plant calculation with a 200% cold-leg break served as the reference transient for the current studies. A comparison between TRAC calculations of the PWR and a corresponding UPTF transient were made. These two are compared in Fig. 15 showing the vessel pressure transient and in Fig. 16 showing the total vessel filling rate. From these studies it was concluded that such integral, or overall parameters, were quite similar between the PWR and the full-scale UPTF. However, a study is still in progress to ascertain the similarities between the detailed multidimensional thermal-hydraulic behavior. We are also proposing a series of separate effects tests, and examining the ability of UPTF to simulate a US design PWR.

In conclusion, the Los Alamos analysis effort is functioning as a vital part of the 2D/3D program. The CCTF and SCTF analyses have demonstrated that TRAC-PF1 can correctly predict multidimensional, nonequilibrium behavior in large-scale facilities prototypical of actual PWR's. Through these and future TRAC analyses the experimental findings can be related from facility to facility; and more importantly, the results of this research program can be directly related to licensing concerns affecting actual PWR's.

TABLE I

SEQUENCE OF EVENTS FOR W PWR LOCA CALCULATION

Event	Time (s)
Transient started:	0.0
Charging pump flow on	0.001
Power decay initiated	0.2
Average rod PCT reached (~775 K)	2.5
Broken loop (Loop 3) accumulator flow started	3.1
SG feedwater flow terminated	4.5
Safety injection flow initiated	5.0
Intact loop accumulator flows initiated (Loops 1, 2, and 4)	13.9-
Charging pump flow terminated	15.0
Initial ECC entry into lower plenum	25.0
Peak intact loop accumulator flows	25-30
End of blowdown	26.1
Lower plenum refilled and reflood begins	36.8
Pressurizer empty	37.0
Broken loop (Loop 3) accumulator liquid flow ended and nitrogen flow begins	47.1
Intact loop accumulator liquid flows ended and nitrogen flow initiated	54-59
Core average rod (outer ring) quenched	70
Core average rod (inner ring) quenched	80
Core completely quenched (all rods)	89

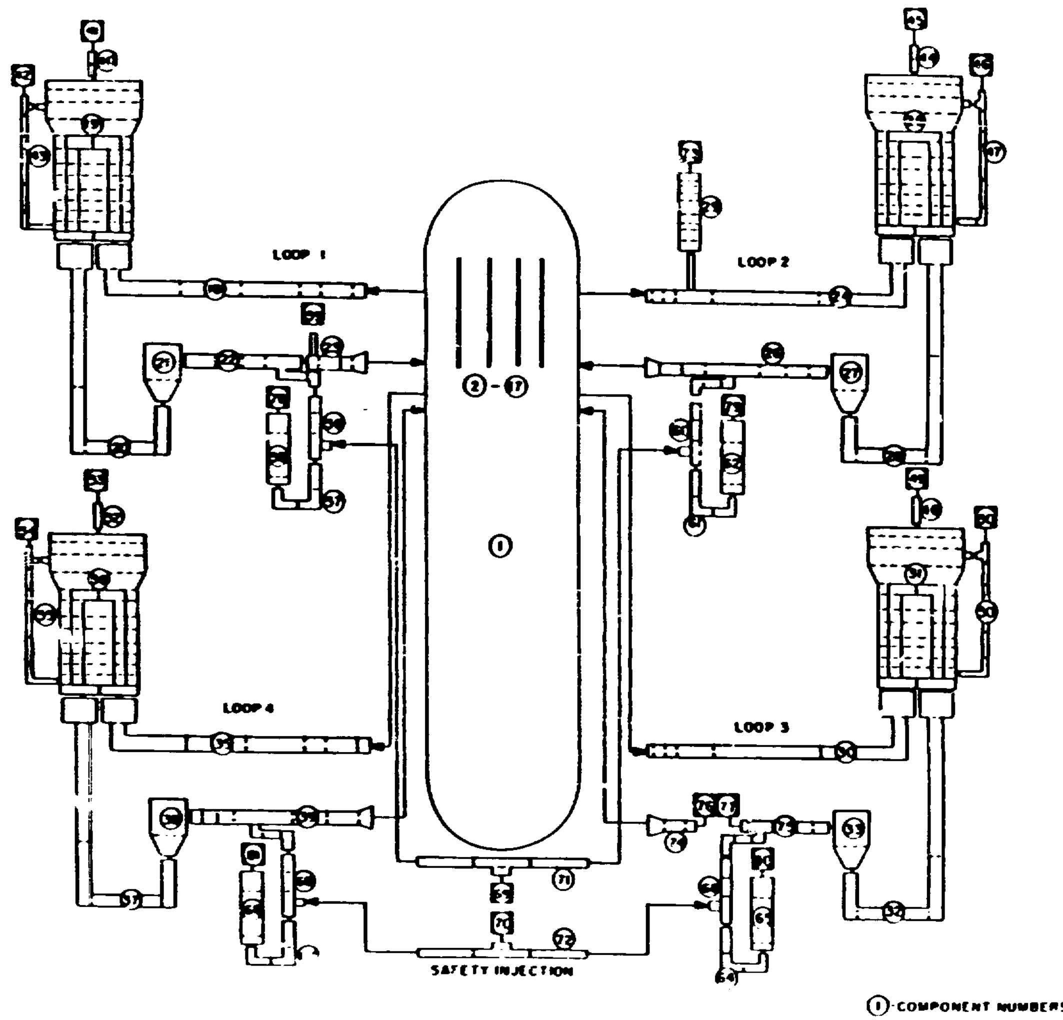

Figure 1. TRAC system model of Westinghouse four-loop PWR

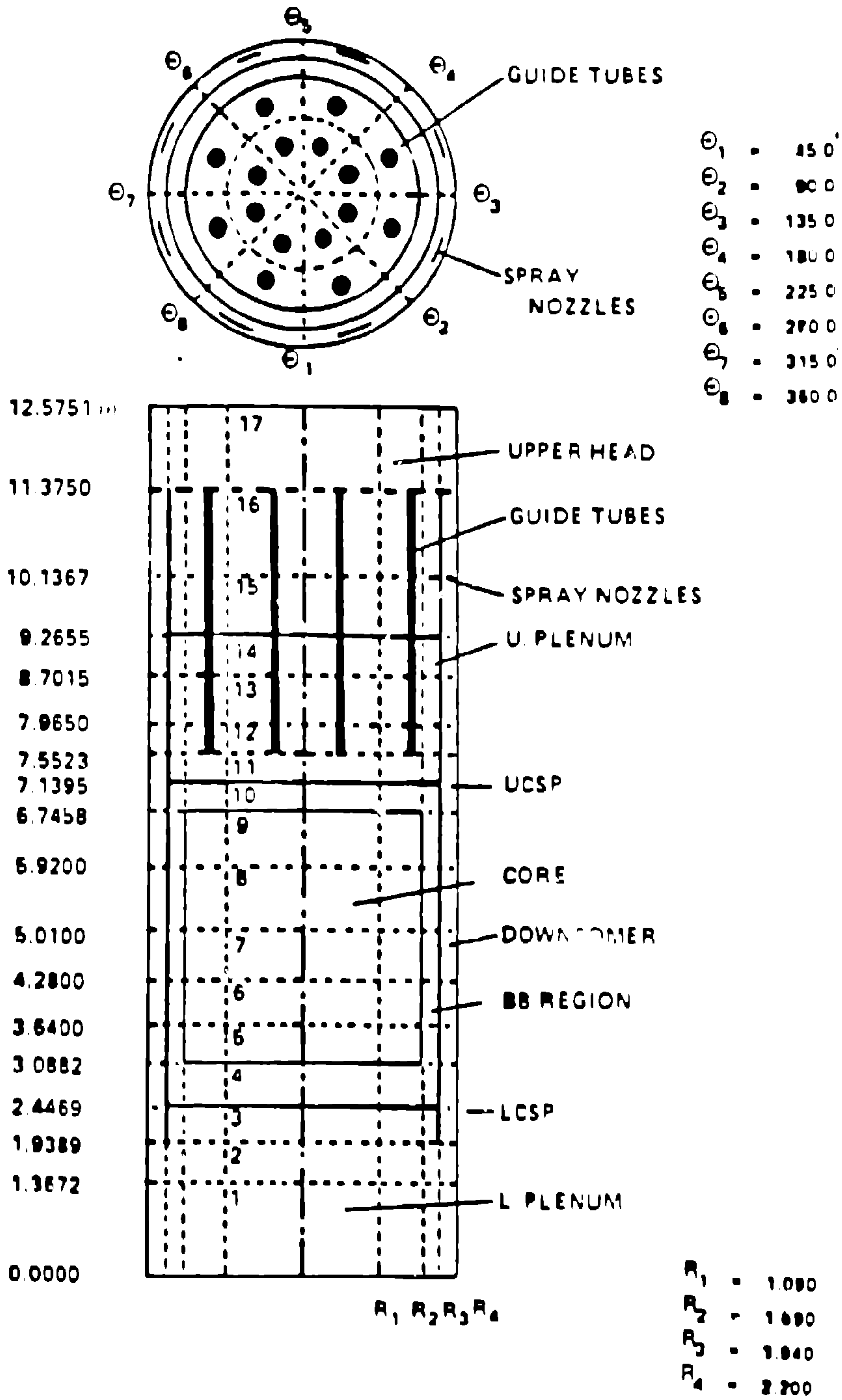

Figure 2. TRAC vessel model of Westinghouse PWR

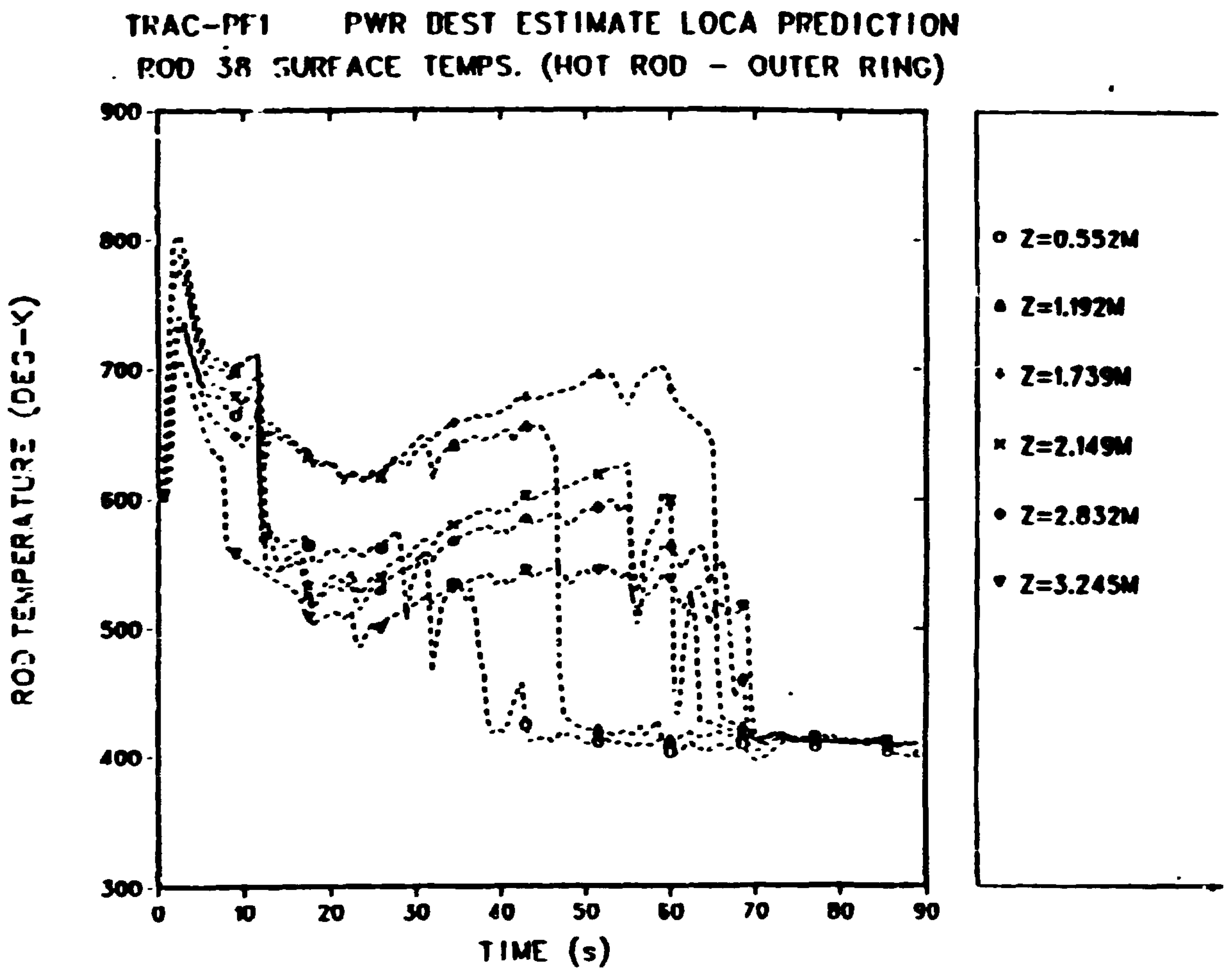

Figure 3. Cladding temperature history of a high powered rod in the Westinghouse LOCA calculation

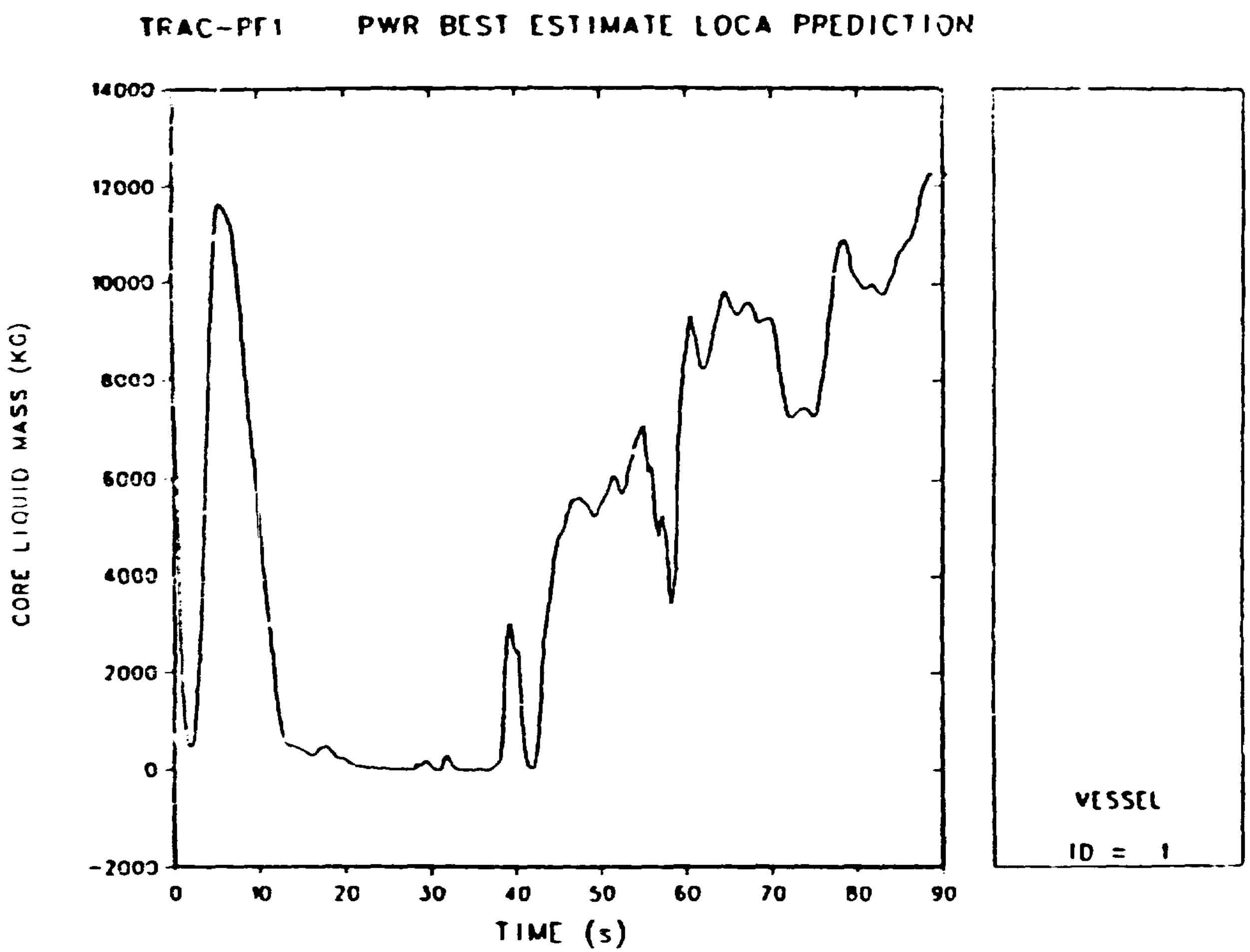

Figure 4. Core liquid mass history in the Westinghouse LOCA calculation

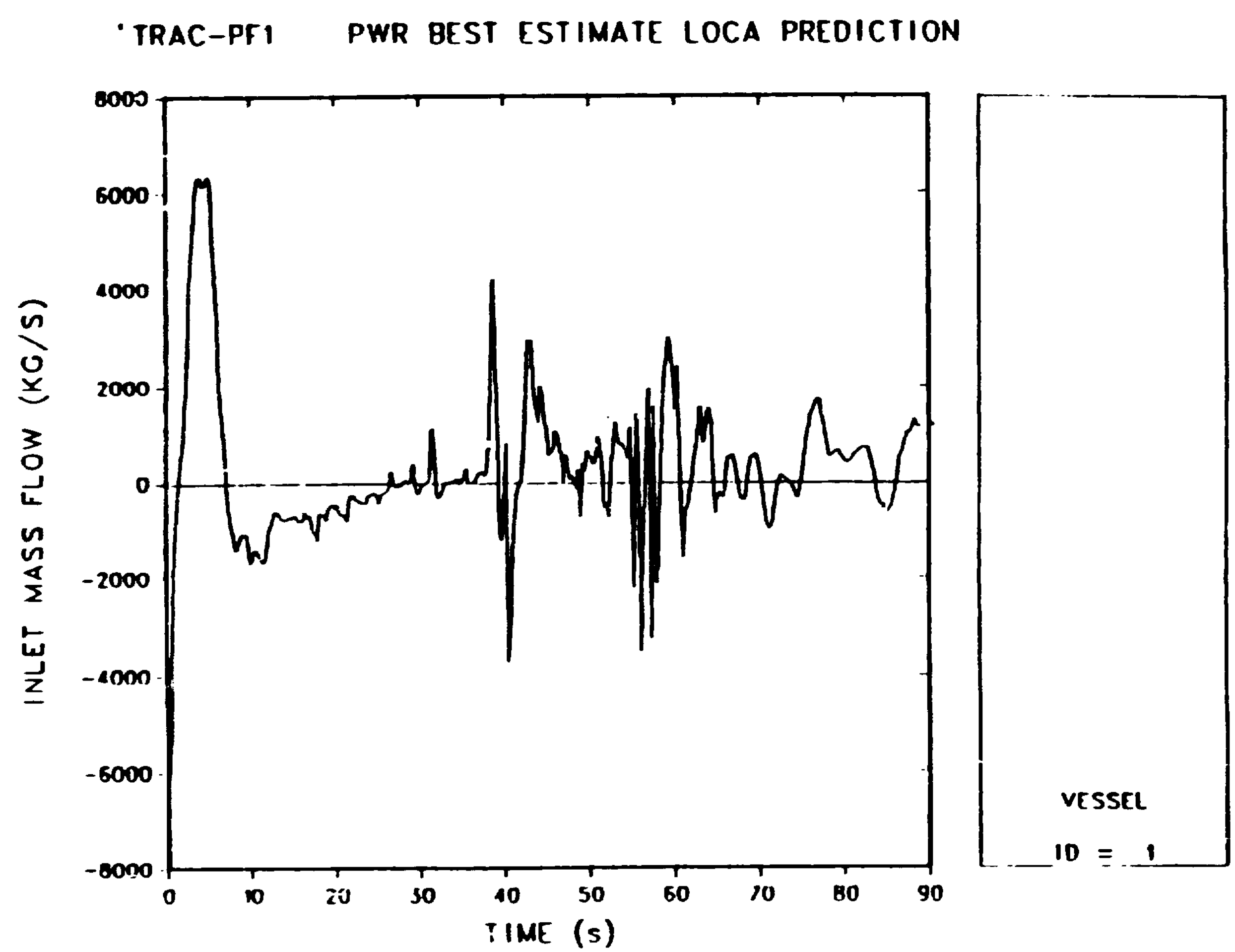

Figure 5. Core inlet mass flow rate in the Westinghouse LOCA calculation

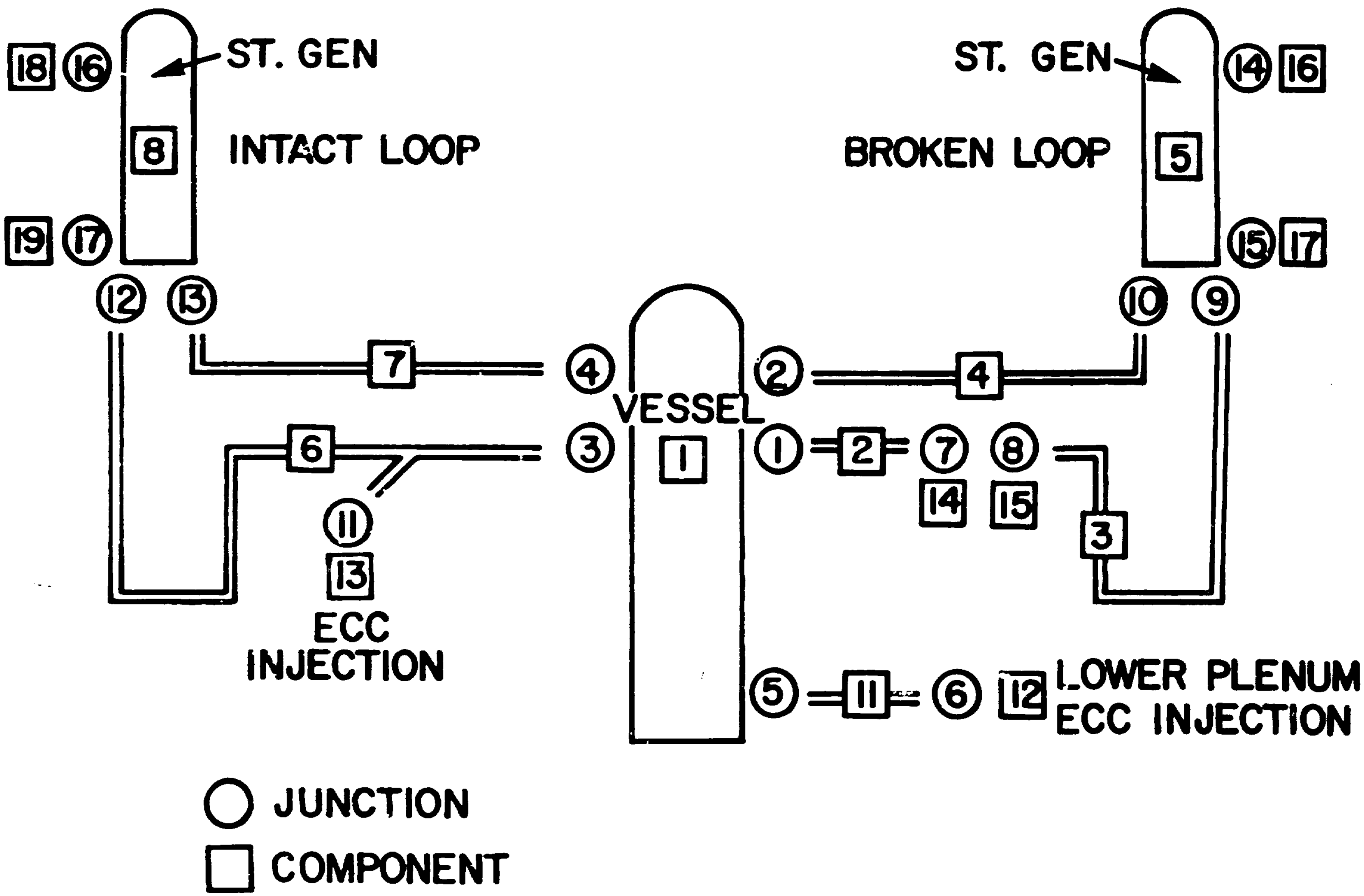

Figure 6. TRAC system model of the Cylindrical Core Test Facility (CCTF)

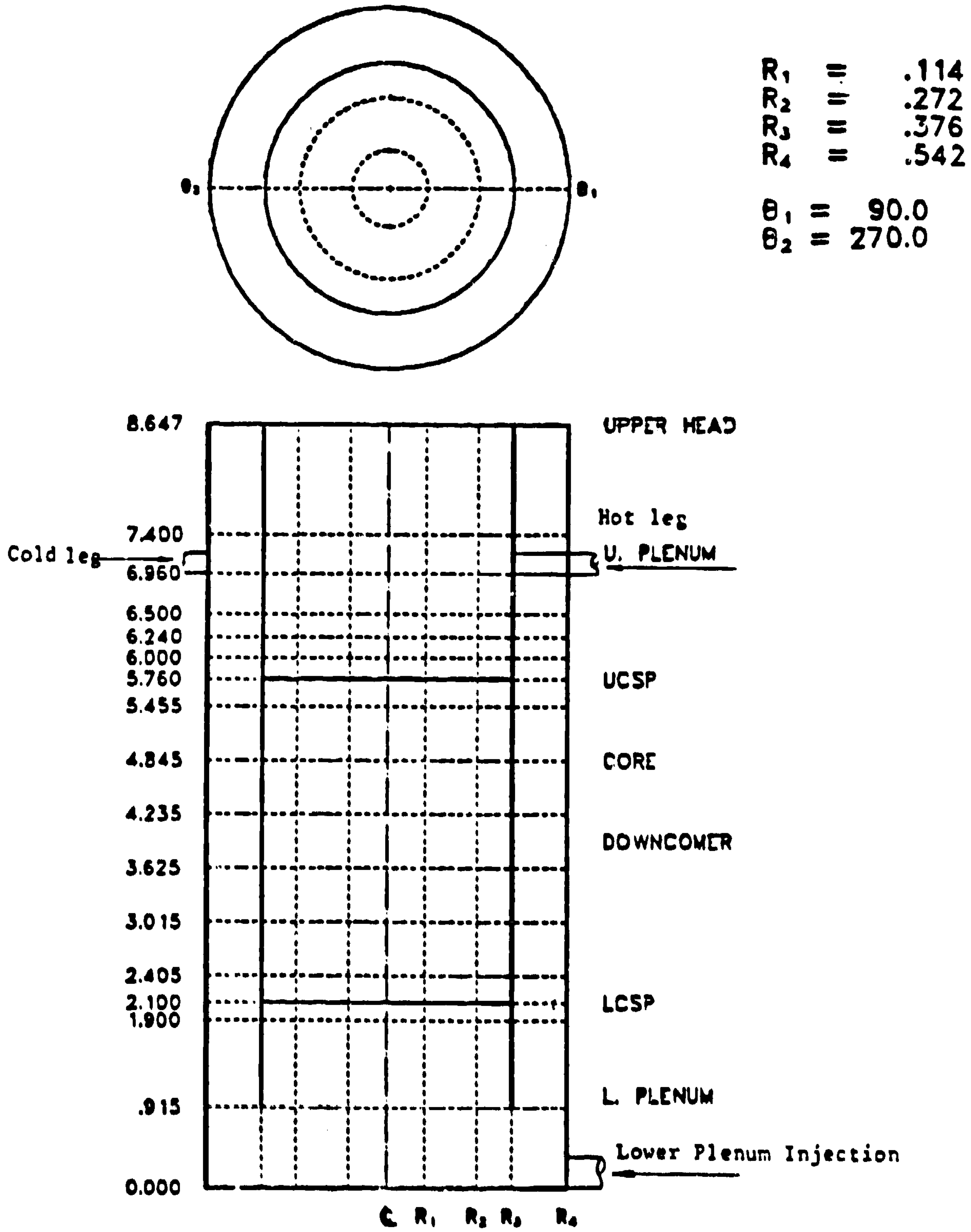

Figure 7. TRAC vessel model of the CCTF

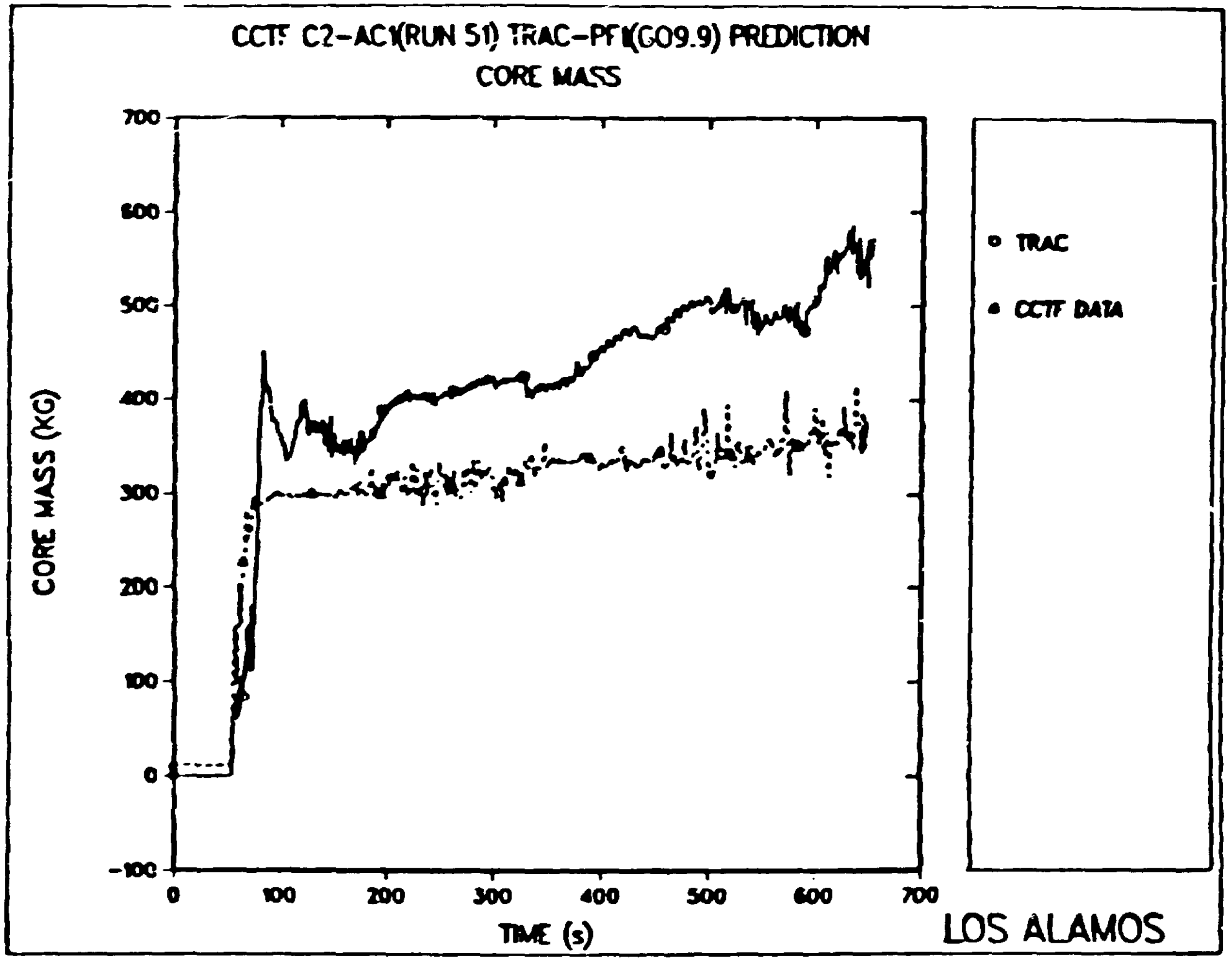

Figure 8. Core liquid mass in the CCTF Run 51

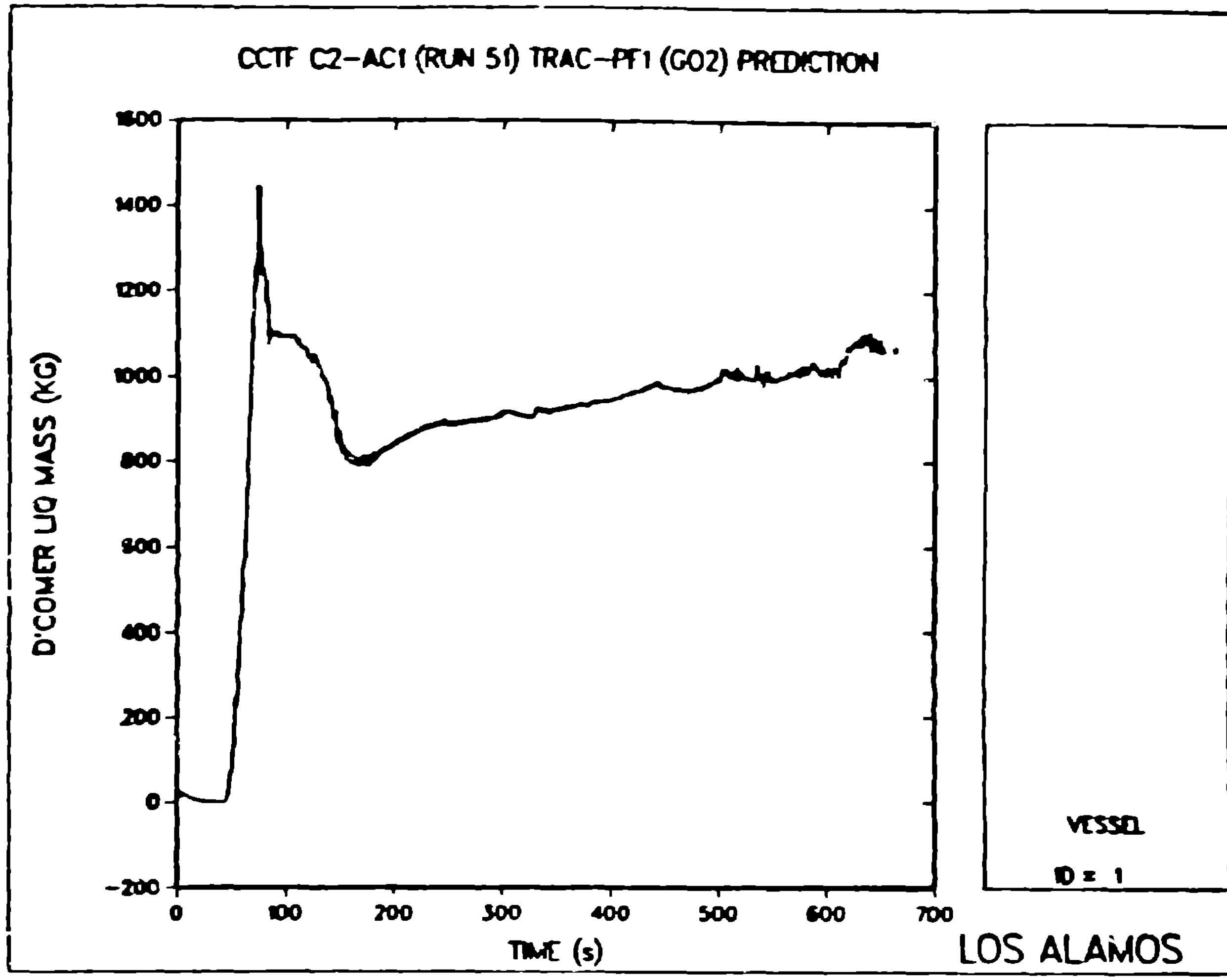

Figure 9. Downcomer liquid mass in the CCTF Run 51

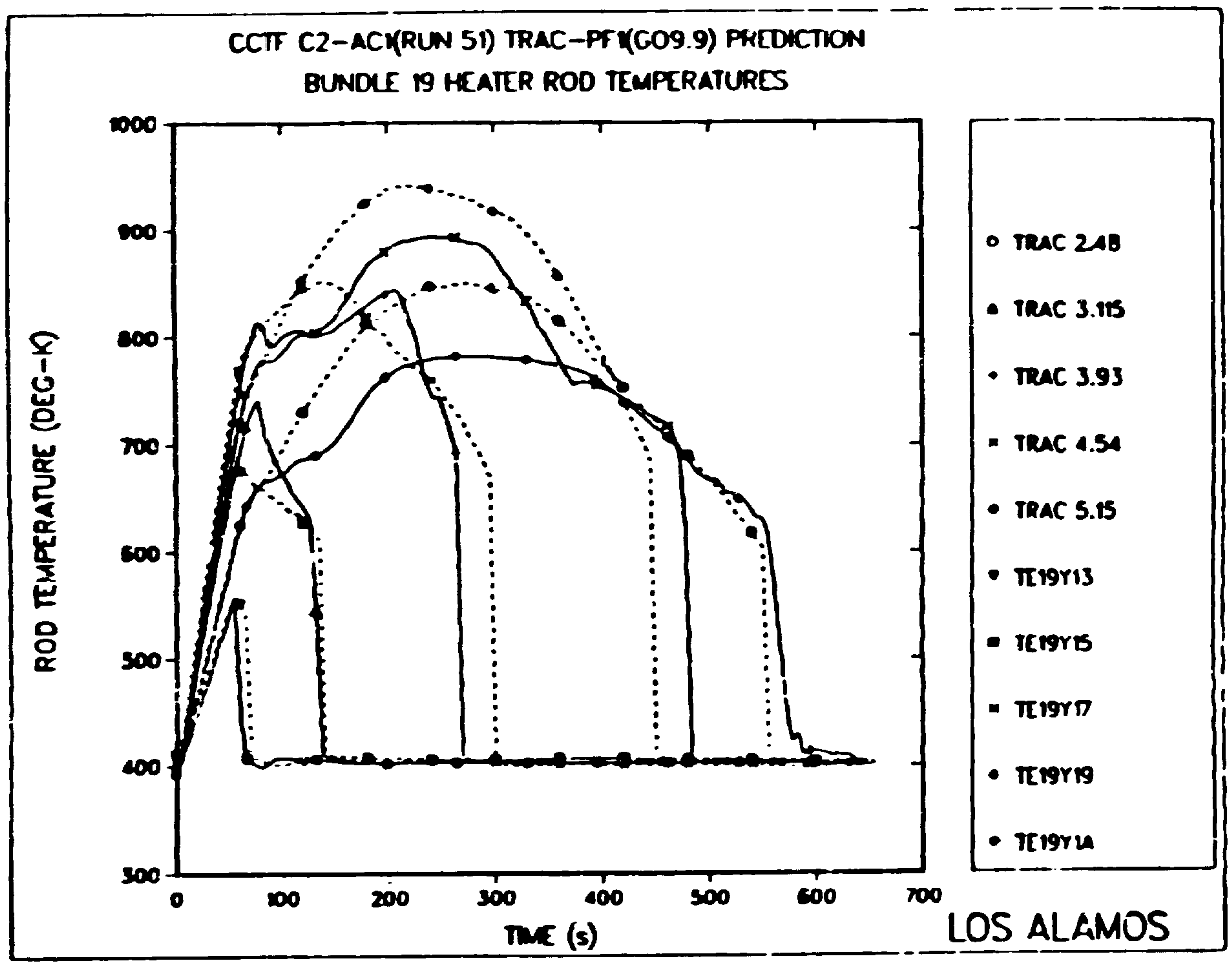

Figure 10. Heater rod thermal response along a medium powered rod in the CCTF Run 51

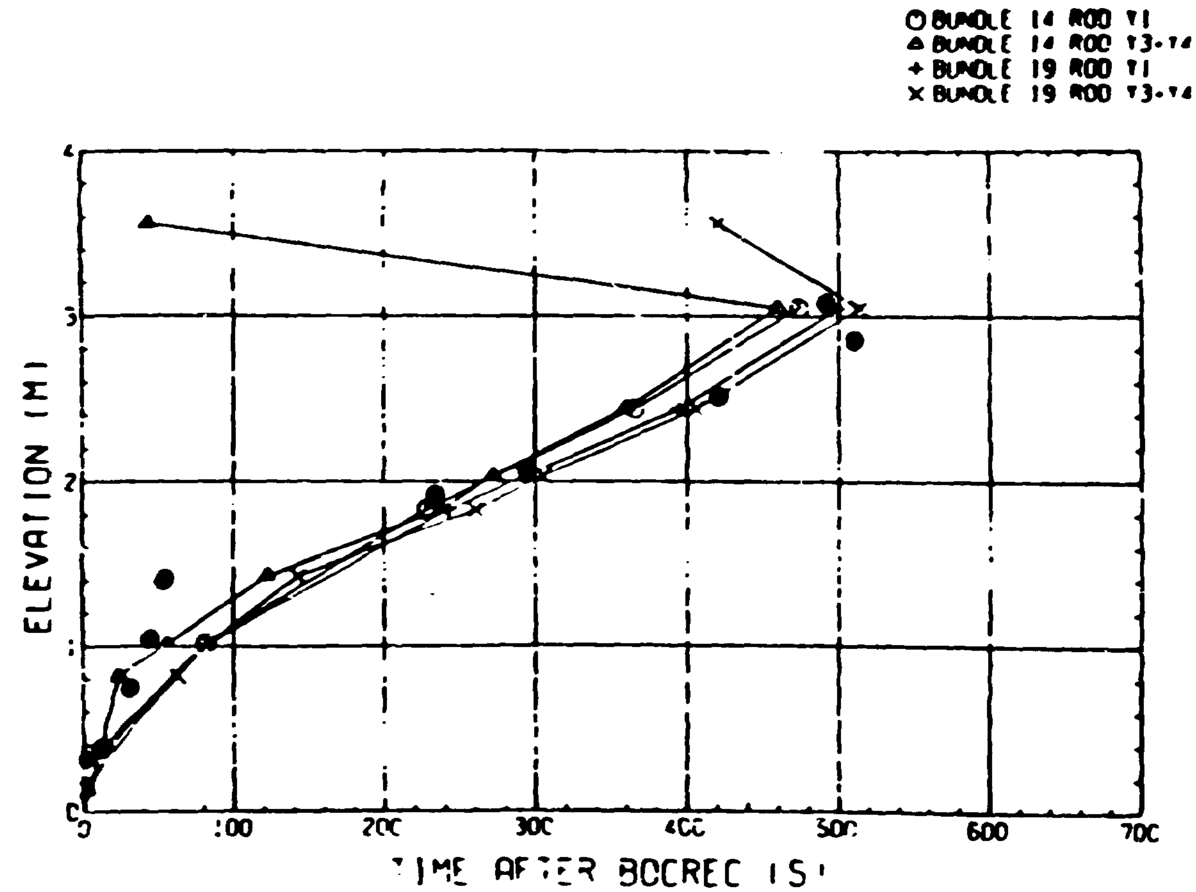

Figure 11. Quench front history along a medium powered rod in the CCTF Run 51.

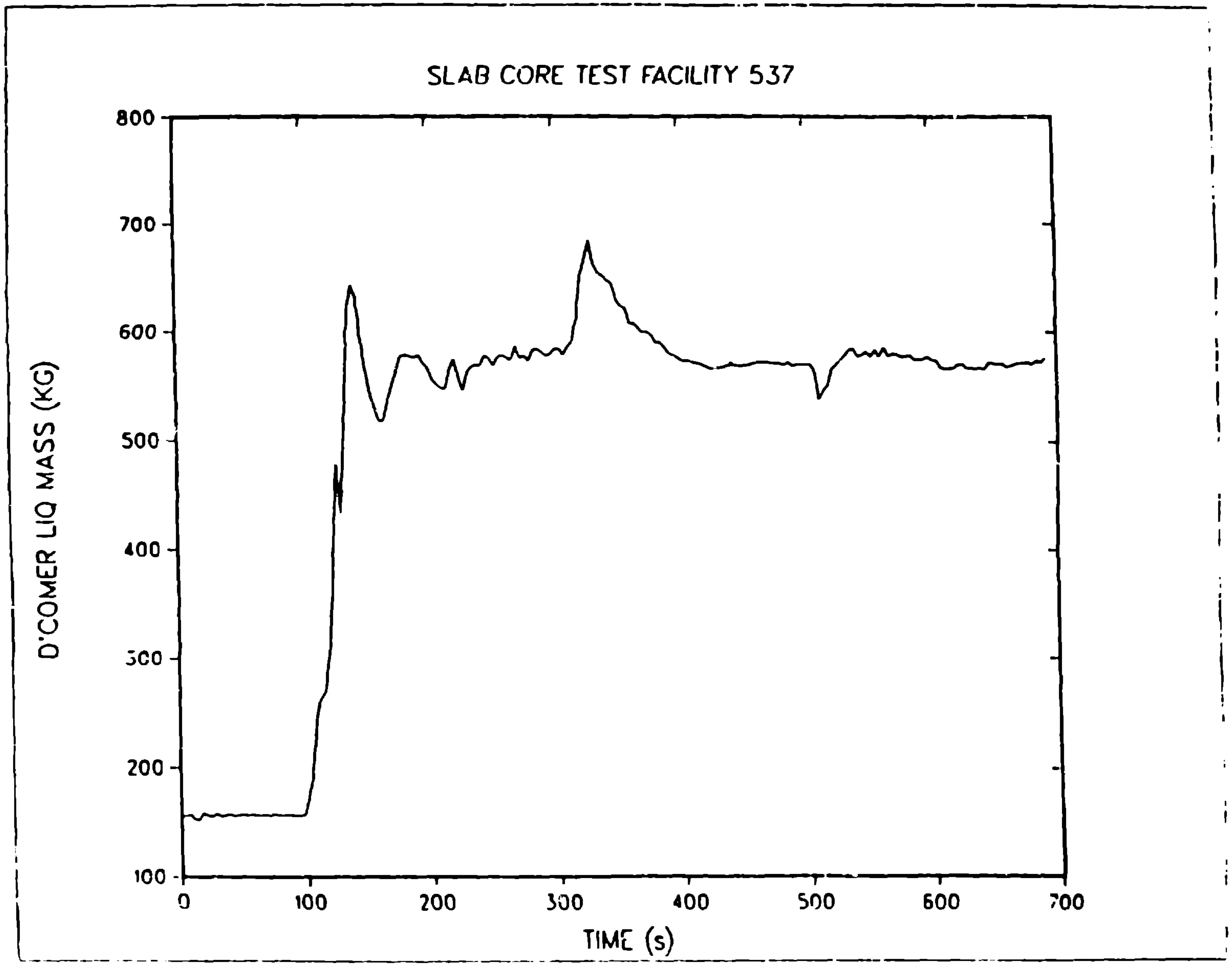

Figure 12. Downcomer liquid mass calculated for the SCTF Run 537

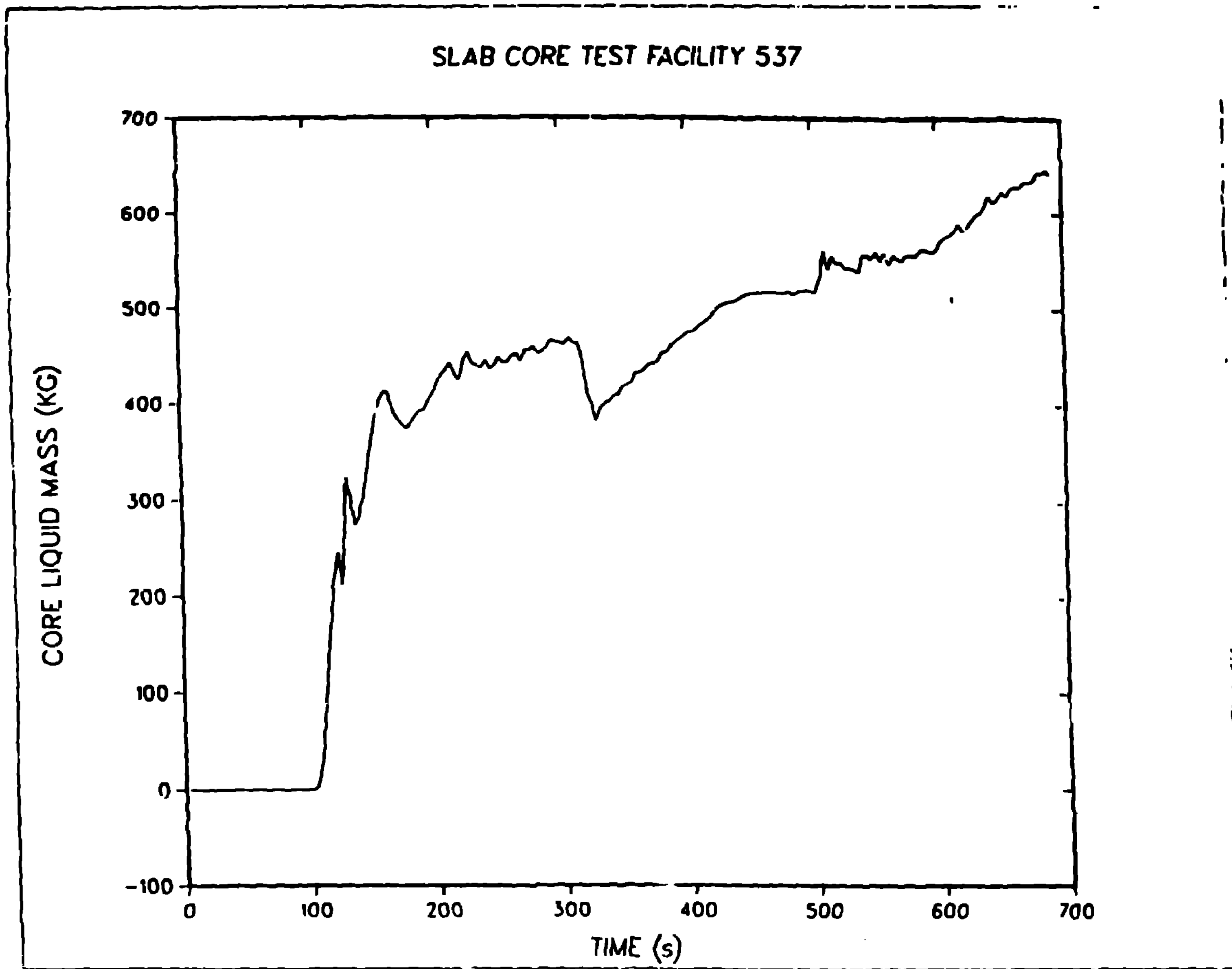

Figure 13. Core liquid mass calculated for the SCTF Run 537

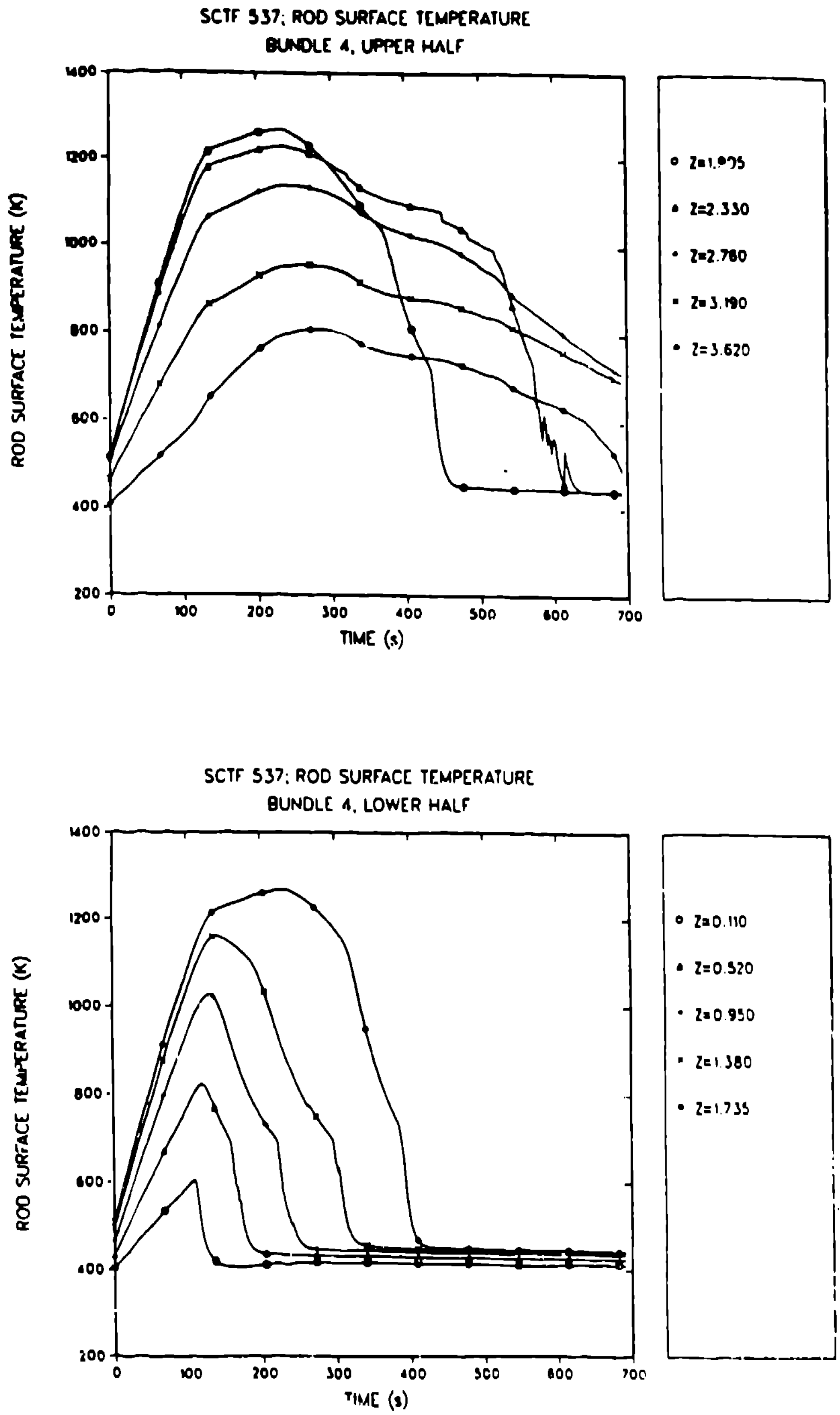

Figure 14. Heater rod thermal response calculated for Bundle 4 in the SCTF Run 537

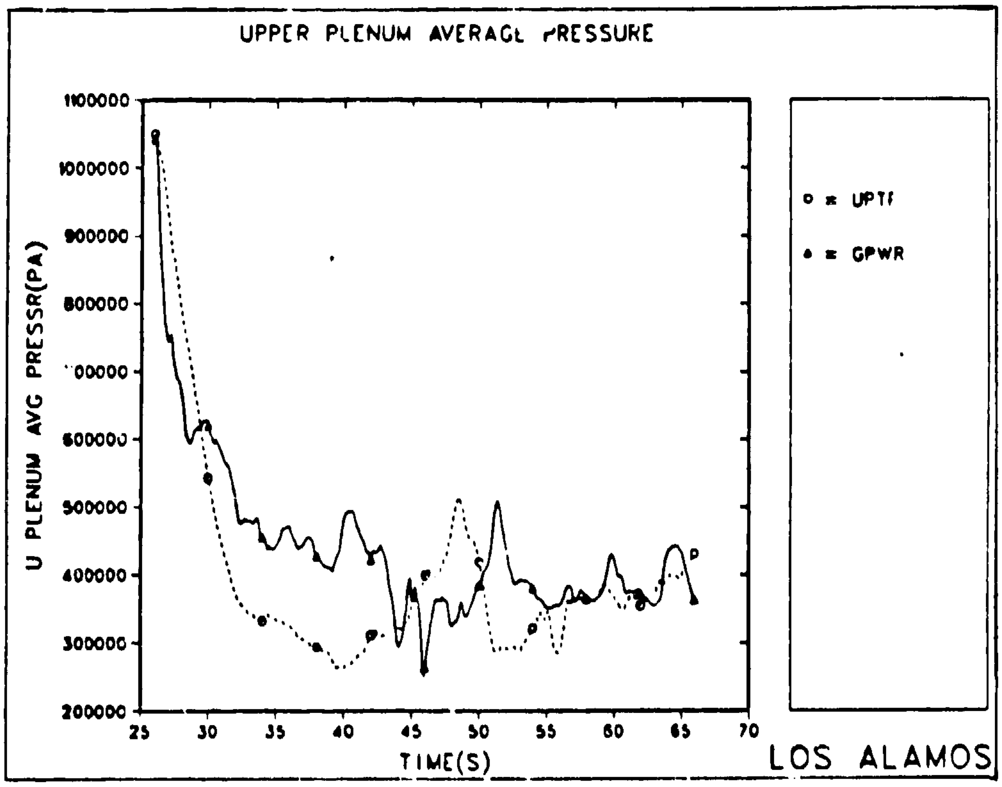

Figure 15. UPTF and GPWR calculated vessel pressure transients

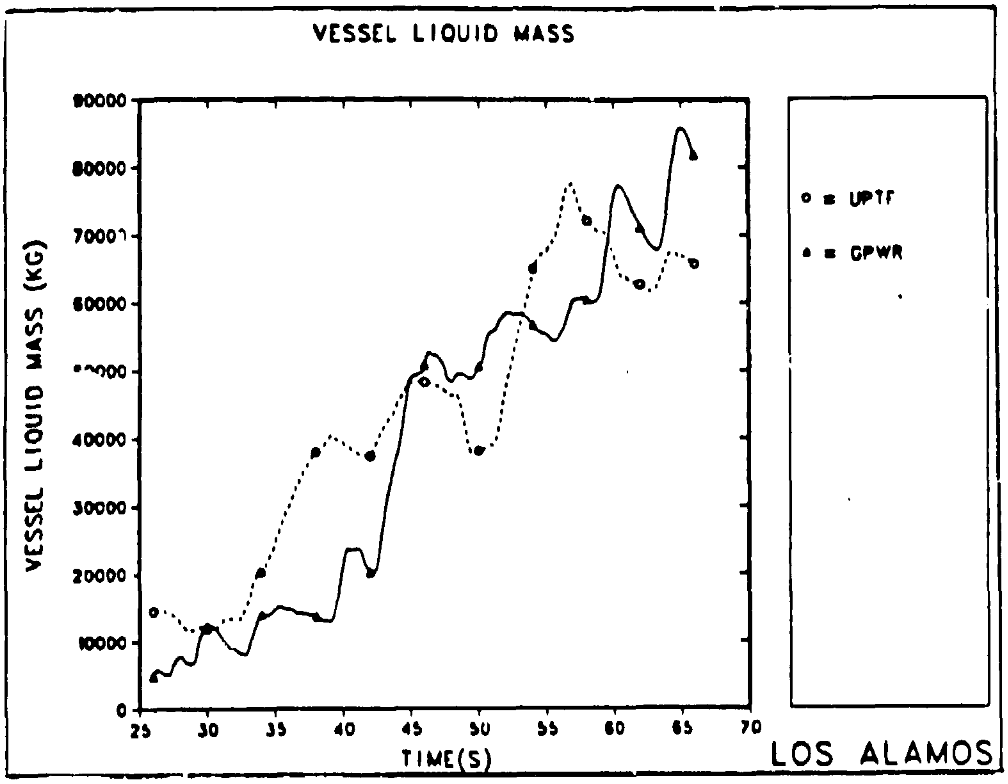

Figure 16. UPTF and GPWR calculated vessel filling rates